TECHNISCHE MECHANIK, Band 20, Heft 1, (2000), 21-29
Manuskripteingang: 19. Juli 1999

From the Spider Leg to a Hydraulic Device

L. Zentner, S. Petkun, R. Blickhan

Workspace and control of multibody systems in nature and engineering are to a large extent determined by the properties of the connecting joints. In contrast to technical joints the natural systems are less stiff incorporating viscoelastic properties and even a simple hinge joint allows for movement and limited control in directions perpendicular to its main plane. Joints of spiders are of special interest as they are driven by hydraulic pressure which may facilitate the construction of micro-devices.
In a first step structure and function of a spider's leg has been investigated simulating movements observed in nature. Following the example from nature a multibody system was developed. Important properties are a) continuity of the material, b) local change of material properties, c) active control of local material properties, and d) hydraulic or pneumatic actuation. The joints can be cascaded thus allowing for the construction of branched multijointed systems driven by a single pressure source. Each joint can be controlled independently. The nonactivated joints remain as stiff as the connected bodies. Thus implementation of such joints do not increase the compliance of the total structure.
In order to facilitate the design we develop a suitable mathematical model including structure, material properties, and control. The model is based on the theory of curved beams with large displacements.

1 Introduction

In animals, a high diversity of joint types can be observed. Major differences are present with their respective degrees of freedom and typical elasticities, which contribute to the adaptivity of the locomotive systems. The hydraulic leg joints of spiders represent an uncommon joint construction, showing both muscular and hydraulic driving mechanisms. With the present paper, an approach is made to reconstruct joints of this kind by the use of technical engineering principles and to transmit the biological functionality into technical joint models.
Spider legs consist of seven segments, connected by different types of joints. Most of the joints are driven by muscles which act either as flexors or as extensors. At the femoro-patellar and tibio-metatarsal joint only flexor muscles are present. The extension is performed by means of hydraulic pressure (Parry, 1959a), (Foelix, 1992).
Like the other arthropods, spiders own an open blood circulation system. The heart is located in the opisthosoma, with the aorta passing through the petiolus to the prosoma. Hemolymph vessels are reaching far into the limbs, with the hemolymph flowing freely back to the opisthosoma. Lacunae in between the muscles and other tissues facilitate the free hemolymph flow. The hemolymph pressure is produced through the contraction of muscles that tend to flatten the prosoma. Also the muscle layers on the opisthosomal body wall play a role in maintaining the hydraulic pressure of the hemolymph (Parry, 1959b), (Wilson, 1970).
Our attention is concentrated on the femoro-patellar and tibio-metatarsal joints, which are examples of a "semi-hydraulic" system. Any flow of the hemolymph in the membraneous area causes a movement of these joints. The axis of rotation of these joints is located at the edge of the segments (Karner, 1998). Under the action of muscles the hemolymph volume in the joint decreases and the membrane is folded. With increasing hemolymph pressure the volume increases and the joint membrane will unfold, thereby tangential forces on the membrane are compensated. Also the pressure force on the membrane does not result in a moment relative to the axes of rotation. Above all, the pressure force of the hemolymph in the joint area is responsible for the rotational movement (Parry, 1959b), (Blickhan, 1983). Only in the areas of structural asymmetry the pressure is not balanced but the torques M_1, M_2 are produced (Figure 1).

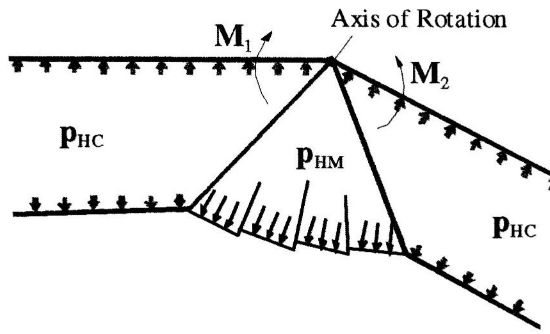

Figure 1. Schematic Representation of a Joint of a Spider, p_{HC} - Hemolymph Pressure onto Cuticle, p_{HM} - Hemolymph Pressure onto Membrane, M_1, M_2 - Bending Moments

This paper aims to understand the construction principle and to transfer it into the technical area. The movement and force producing principles of a spider leg can serve as a basis for hydraulic drives for micro manipulators. The fast progress in micro technique leads to new construction solution through new materials and technology. In the micro technique hydraulic drives occupy a leading role. Just in this connection, the movement principle of a spider's leg offers favourable and innovative constructive solutions.

2 Possible Technical Realisation of Hydraulic Joints

Some principles of material-constraint joints with a hydraulic drive are shown in the following figures (Figure 2-3). The joints, material coherent joints with spatially fixed invariable flexibility, are shown as asymmetric constructions and can be driven by hydraulics or pneumatics. They can be realized a) as a segment of a body, that has less resistance to bending e.g. through reduction of the material (Figure 2a)); b) as a segment of a body with less density than the remaining parts of the body e.g. through an asymmetrically arranged opening or an asymmetric interior (Figure 2b)-c)); c) as a segment of a body with a different anisotropy than the remaining areas of the body e.g. through the embedding of another body (Figure 2d)).
Material coherent joints with controllable variable flexibility are built symmetrically (Figure 3). The material has mechanical reversible properties (stiffness). Through local asymmetrical perturbation of the material, the change of pressure produces a movement. Constructive-morphologically there are two ways to produce movement: 1) Embedding some asymmetry into the construction (Figure 2) or 2) asymmetrical supply of energy into a symmetrical construction (Figure 3).

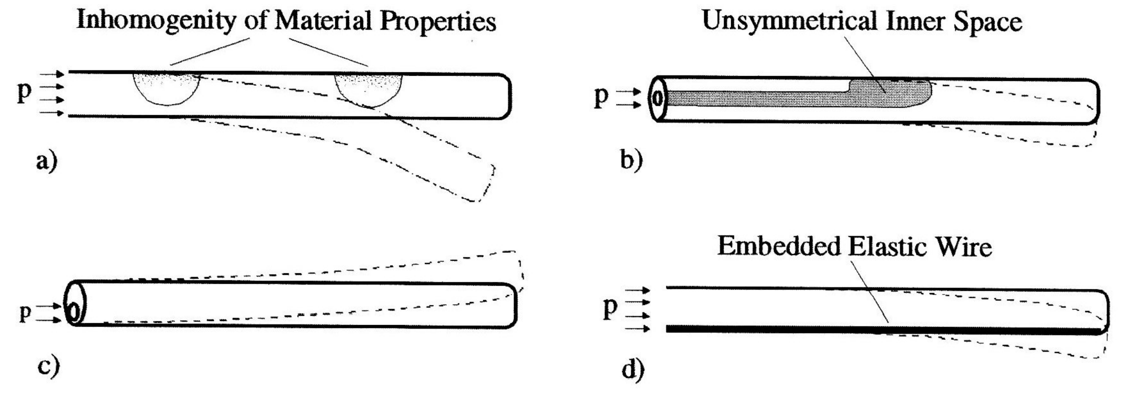

Figure 2. Material Coherent Joints with Spatially Fixed Invariable Flexibility

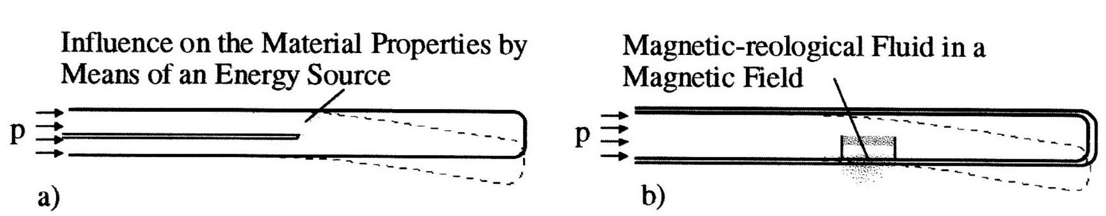

Figure 3. Material Coherent Joints with Controllable Variable Flexibility: Reversible Effect on the Material at a Desired Place with the Aim to Create a Joint

According to the shown principles (Figure 3a) a pattern was made. The material properties of polymer tubes are changed through the local effect of a heating source. The material becomes more compliant at the warmed location. The compliant area is extended through increasing pressure in the tube. That leads to an alteration of the form. The given form of the tube will remain after cooling down. The original form of the tube can be restored through the renewed warming of the tube and by applying pressure. Such joints can be used as monolithic cascade structures and separately controlled. A finger with material coherent joints is shown in the Figure 4. The "finger" is driven pneumatically.

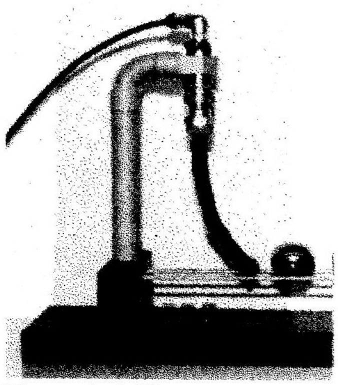

Figure 4. A Finger with Material Coherent Joints

3 A Mathematical Model

To facilitate the design of such structures, it is necessary to set up a suitable mathematical model. For a joint with embedded material (Figure 2d) such a model is studied. The analysis of the model helps to understand the behaviour and the stability of the joints taking into account the material properties. The model is based on the theory of curved beams. Another approach to a similar problem is developed in (Lauschke, 1997).

The following assumptions from classical beam theory are valid (Love, 1927), (Svetlickii, 1987):

1) The normal cross-sections of a beam, plane before deformation, remain normal and plane after deformation (Bernoulli hypothesis), i.e. shear deformations are not taken into account;
2) The sizes of cross-section are small in comparison with the length and the radius of curvature of a beam;
3) Lines parallel to the axial line keep their lengths;
4) St.Venant's principle holds, which says, that various, but statically equivalent, local loads produce the same stresses in the beam.

In connection with the assumption that the material of a beam satisfies Hooke's law, the solutions of problems must be accepted only if the maximum normal stresses, arising in a beam, remain below the limit of proportionality for a given material.

We introduce two orthogonal systems of coordinates: stationary Cartesian (fixed) ones with unit vectors $\mathbf{e}_{j0}$ and mobile ones with unit vectors $\mathbf{e}_j$ (Figure 5), attached to the neutral line. The distance between the neutral line and the center of mass is h .

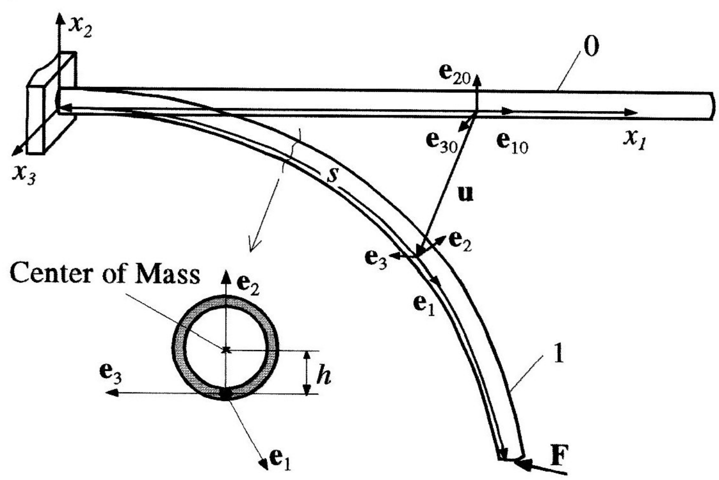

Figure 5. Two State of the Beam: 0 – Unloaded, 1 – Loaded

The length of an arch s of the neutral line is measured from the fixed end to the free end. Under the action of slowly increasing forces and moments (is considered static) the beam, being deformed, transforms from state 0 into state 1. The elastic displacements can be so large, that the form of an axial line of the beam strongly differs from its initial course. External forces also noticeably change their direction during deformation of the beam. For the solution of the nonlinear static problems of flexible beams it is necessary to know the behaviour of external loads during deformation. The flexible beams will have different final forms, if, for example, a beam is loaded in one case "stationary" by force (i.e. - the load does not change its direction and magnitude in the process of deformation and in another - "following" - the force keeps its direction in relation to the beam during deformation and will have a constant angle with the mobile axes.

Derivation of Vector Equations of Equilibrium of a Beam.

We consider an element of a beam of length ds (Figure 6a). The following designations are chosen: $\mathbf{Q}$ - vector of internal forces, which is equal to $\mathbf{Q} = Q_1\mathbf{e}_1 + Q_2\mathbf{e}_2 + Q_3\mathbf{e}_3$, where Q_1 - axial force, Q_2 and Q_3 - transverse forces; $\mathbf{M} = M_1\mathbf{e}_1 + M_2\mathbf{e}_2 + M_3\mathbf{e}_3$ - vector of internal moments, where M_1 - torsional moment, M_2 and M_3 - bending moments.
We consider a separate element of a beam (Figure 6b) and of a gasfilled pipe (Figure 6a) with all forces, acting on them.
Using d'Alembert's principle, one can obtain the following equation:

$$-\frac{d(P_0\mathbf{e}_1)}{ds}-\mathbf{f} = \mathbf{0} \qquad P_0 = pA_a \tag{1}$$

where A_a - area of cross-section of a beam (pipe), p - pressure of gas, $\mathbf{f}$ - distributed force of interaction of the pipe with gas.
For a beam element it is possible to derive the following equation of equilibrium with glance to the gravitational forces of a beam:

$$d\mathbf{Q} + \mathbf{f}ds + d(m\mathbf{g}) = \mathbf{0} \tag{2}$$

Eliminating vector $\mathbf{f}$ from equations (1) and (2), we obtain:

$$\frac{d\mathbf{Q}}{ds} - \frac{d(p_0\mathbf{e}_1)}{ds} + \mathbf{q} = \mathbf{0}$$

$$\mathbf{q} = \frac{d(m\mathbf{g})}{ds} \tag{3}$$

The equation of equilibrium of moments, acting on an element of a beam, can be written as

$$\frac{d\mathbf{M}}{ds} + (\mathbf{e}_1 \times \mathbf{Q}) + (h\mathbf{e}_2 \times \mathbf{q}) = \mathbf{0} \tag{4}$$

For solving of a static problem it is not sufficient to determine $\mathbf{Q}$ and $\mathbf{M}$, it is necessary to know the deformation of a beam, which is determined by the local curvature $\boldsymbol{\kappa}$.

Equation, Connecting Vectors M and κ

We consider a beam element in the deformed state described in the mobile system of coordinates. The projection of an axial line has the curvatures κ_2 and κ_3 in planes passing through major axes of the section. They are projections of curvature of a axial line in space.

Assuming, that the moment M_1, M_2 and M_3 are proportional to the changes of curvature of an axial line of a beam and torsion, one can write three equations:

$$\mathbf{M}_i = A_{ii}(\boldsymbol{\kappa}_i - \boldsymbol{\kappa}_{i0}) \qquad i=\overline{1,3} \tag{5}$$

where $\boldsymbol{\kappa}_{i0}$ - torsion and curvatures before deformation. In our case $\boldsymbol{\kappa}_{io} = \mathbf{0}$, since the initial state of a beam is straight, A_{ii} - are the stiffnesses under torsion and bending, which depend on s and can be given by:

$$A_{11} = GJ_k\,;\; A_{22} = EI_2\,;\; A_{33} = EI_3$$

where E, G - Young's modulus and shear modulus; I_2, I_3 - moments of inertia of cross-section of a beam with respect to the major axes, passing through a point O, J_k - moment of inertia of the cross-section under torsion. The rather simple dependence (5) of internal moment $\mathbf{M}_i$ from increments of $\boldsymbol{\kappa}_i$ is possible only in natural coordinates. The system of equations (5) can be expressed in term of one vector equation (in basis $\mathbf{e}_j$)

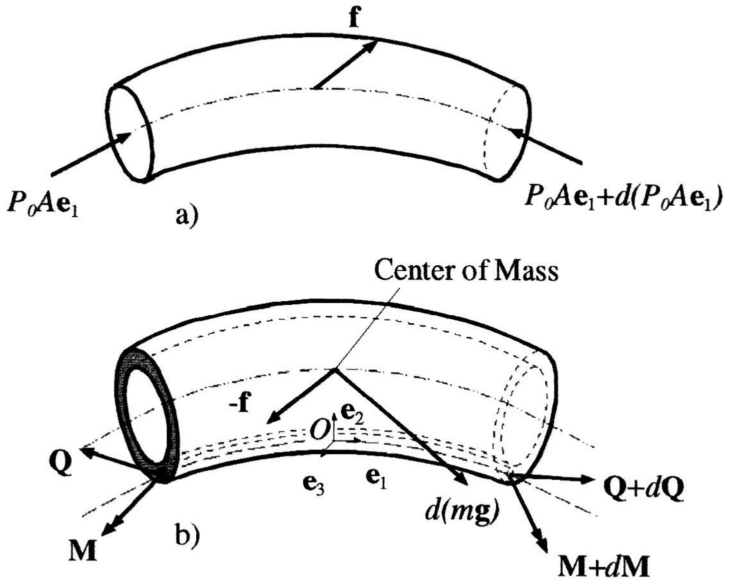

Figure 6. An Element of the Beam, Filled with Gas: a) - Element of Gas, b) - Element of the Pipe

$$\mathbf{M} = \mathbf{A}\boldsymbol{\kappa} \qquad \boldsymbol{\kappa}_i = \kappa_i \mathbf{e}_i \tag{6}$$

where
$$\mathbf{A} = \begin{bmatrix} A_{11} & 0 & 0 \\ 0 & A_{22} & 0 \\ 0 & 0 & A_{33} \end{bmatrix}$$

The equations (3), (4) and (6) are nonlinear equations of equilibrium and constitutive equations of a linear beam, when a neutral line of a loaded beam is a space curve:

$$\begin{cases} \dfrac{d\mathbf{Q}}{ds} - \dfrac{d(P_0\mathbf{e}_1)}{ds} + \mathbf{q} = \mathbf{0} \\ \dfrac{d\mathbf{M}}{ds} + (\mathbf{e}_1 \times \mathbf{Q}) + (h\mathbf{e}_2 \times \mathbf{q}) = \mathbf{0} \\ \mathbf{M} = \mathbf{A}\boldsymbol{\kappa} \end{cases} \tag{7}$$

Equations in dimensionless form we obtain by substituting:

$$\begin{array}{llll} s = l\varepsilon & \mathbf{Q} = \dfrac{\tilde{\mathbf{Q}}A_{33}(0)}{l^2} & \mathbf{M} = \dfrac{\tilde{\mathbf{M}}A_{33}(0)}{l} & P_0 = \dfrac{\tilde{P}_0A_{33}(0)}{l^2} \\ h = \tilde{h}\varepsilon & \mathbf{q} = \dfrac{\tilde{\mathbf{q}}A_{33}(0)}{l^3} & A_{ii} = \tilde{A}_{ii}A_{33}(0) & \boldsymbol{\kappa} = \dfrac{\tilde{\boldsymbol{\kappa}}}{l} \end{array} \tag{8}$$

After transformations for a beam with constant cross-section we get the following system of equations (tilde for dimensionless quantities is omitted):

$$
\begin{cases}
\dfrac{d\mathbf{Q}}{d\varepsilon} + \mathbf{q} = \mathbf{0} \\
\dfrac{d\mathbf{M}}{d\varepsilon} + (\mathbf{e}_1 \times \mathbf{Q}) + (h\mathbf{e}_2 \times \mathbf{q}) = \mathbf{0} \qquad \text{Here:} \quad \mathbf{Q} = (Q_1 - P)\mathbf{e}_1 + Q_2\mathbf{e}_2 + Q_3\mathbf{e}_3 \\
\mathbf{M} = \mathbf{A}\boldsymbol{\kappa}
\end{cases} \tag{9}
$$

Equations of Equilibrium in Projections on Attached Axes

To obtain the equation system in the projections on coordinate axes, it is necessary to keep in mind, that not only the projections of appropriate vectors depend on ε, but also individual vectors $\{\mathbf{e}_i(\varepsilon)\}$ are functions of ε. In equations (9) we use local derivatives:

$$
\begin{cases}
\dfrac{d\mathbf{Q}}{d\varepsilon} + (\boldsymbol{\kappa} \times \mathbf{Q}) + \mathbf{q} = \mathbf{0} \\
\dfrac{d\mathbf{M}}{d\varepsilon} + (\boldsymbol{\kappa} \times \mathbf{M}) + (\mathbf{e}_1 \times \mathbf{Q}) + (h\mathbf{e}_2 \times \mathbf{q}) = \mathbf{0} \\
\mathbf{M} = \mathbf{A}\boldsymbol{\kappa}
\end{cases} \tag{10}
$$

In our particular problem the beam deformations occur in the plane $\{x_1, x_2\}$. That is why only the basic vectors $\mathbf{e}_1$ and $\mathbf{e}_2$ remain in the equations. If a neutral line of a loaded beam is a planar curve ($\kappa_1 = \kappa_2 = 0$), then equations of a linear beam are:

$$
\begin{cases}
\mathbf{e}_1 : \dfrac{dQ_1}{d\varepsilon} - Q_2\kappa_3 + q_1 = 0 \\
\mathbf{e}_2 : \dfrac{dQ_2}{d\varepsilon} + Q_1\kappa_3 + q_2 = 0 \\
\mathbf{e}_3 : \dfrac{dM_3}{d\varepsilon} + Q_2 + hq_1 = 0 \\
M_3 = A_{33}\kappa_3
\end{cases} \tag{11}
$$

This system of nonlinear equations was solved with the program MATHEMATICA with boundary conditions:

$$
Q_1(l) = 0 \qquad Q_2(l) = Fl^2/A_{33} \qquad \kappa_3(0) = 0 \tag{12}
$$

with the following data for the beam (Figure 7):

$$
\begin{aligned}
&l = 88.2\text{ mm}; \quad p = (1+0.1\,i)\text{ bar}, i=0,\dots,5; \quad h = 3.4\text{ mm} \\
&A_{33} = 0.02\text{ Nm}; \quad A_a = 12.57\text{ mm}^2; \quad F = 10\text{ N}
\end{aligned} \tag{13}
$$

The gravity force acting on the beam, was not taken into account ($q_i = 0$). The beam is loaded with sufficient pressure, to help the force acting on it remains in this case without changing. It is important to compare the theoretical results with measurements on the real object. The measurements were made either with constant pressure or with constant force. The comparison between calculated and experimental results is shown in Figure 8. The maximum deviation between the measured and calculated displacements is about 12% for variable pressure and 5% for variable force.

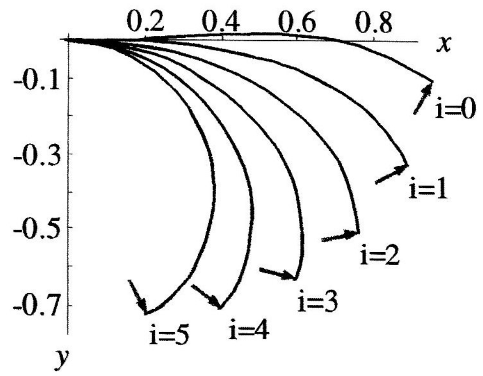

Figure 7: The Calculated Results: Changing of the Beam Form under the Increasing Pressure

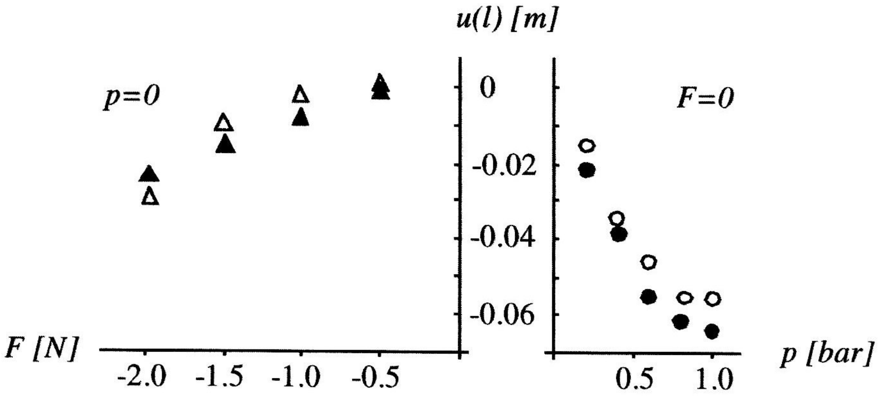

Figure 8: Comparison between Calculated Results (filled marks) with the Measured Results (blank marks)
Displacement of the Beam End as Function of Force (left) and Pressure (right)

Study of Stability of Beams

If small perturbations of loads, acting on the beam, cause a jump from one stable state to a different stable state of equilibrium we have a stability problem. This sudden transition from one state of equilibrium to a different one is called the loss of static stability of a beam. For finding linear equations of equilibrium of a beam after loss of stability we assume:

$$\mathbf{Q} = \mathbf{Q}_* + \mathbf{Q}_0 \qquad \mathbf{M} = \mathbf{M}_* + \mathbf{M}_0 \qquad \mathbf{q} = \mathbf{q}_* + \Delta\mathbf{q}_0 \qquad \boldsymbol{\kappa} = \boldsymbol{\kappa}_* + \Delta\boldsymbol{\kappa} \tag{14}$$

where vectors assigned by an asterisk * are appropriate for the moment of loss of stability; Q_0, M_0, $\Delta\kappa$, Δq - increments of appropriate vectors at transition of a beam into the buckled equilibrium state. Only small increments take place. We consider two states of a beam element (Figure 9): 0 - critical and 1 - buckled state.
In state 1, i.e. in basis $\{\mathbf{e}_i\}$, the vectors with asterisk * are of the form (for example, $\mathbf{Q}_*^1$ and $\mathbf{M}_*^1$)

$$\mathbf{Q}_*^1 = \sum_{j=1}^{3} Q_{*j}\mathbf{e}_j$$

$$\mathbf{M}_*^1 = \sum_{j=1}^{3} M_{*j}\mathbf{e}_j$$

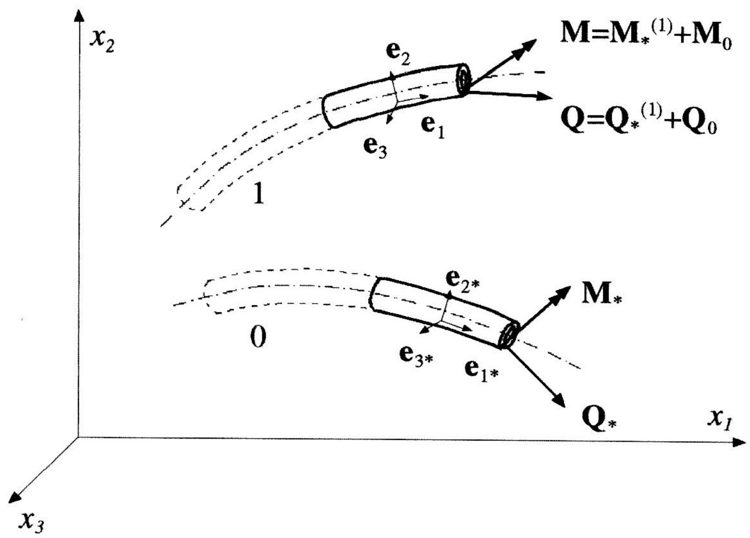

Figure 9: The Beams: 0 - Critical State, 1 - Buckled Position

where Q_{*j} and M_{*j} are projections of vectors onto the basis $\{\mathbf{e}_j\}$, therefore $Q_*^{(1)} \neq Q_*, M_*^{(1)} \neq M_*$
We substitute expressions (14) into equations (10) and linearize them by increments.

$$
\begin{cases}
\dfrac{d\mathbf{M}_0}{ds} + (\Delta\boldsymbol{\kappa}\times\mathbf{M}_*^{(1)}) + (\boldsymbol{\kappa}_*^{(1)}\times\mathbf{M}_0) + (\mathbf{e}_1\times\mathbf{Q}_0) + (h\mathbf{e}_2\times\Delta\mathbf{q}) = \mathbf{0} \\
\dfrac{d\mathbf{Q}_0}{ds} + (\Delta\boldsymbol{\kappa}\times\mathbf{Q}_*^{(1)}) + (\boldsymbol{\kappa}_*\times\mathbf{Q}_0) + \Delta\mathbf{q} = \mathbf{0} \\
\mathbf{M}_0 = \mathbf{A}\Delta\boldsymbol{\kappa}
\end{cases}
\tag{15}
$$

For rectilinear beam the linear equations (15) in projections on mobile coordinates axes are:

$$
\begin{cases}
\mathbf{e}_1 : \dfrac{dQ_{01}}{d\varepsilon} - Q_{2*}\dfrac{M_{03}}{A_{33}} - \kappa_{3*}Q_{02} + \Delta q_1 = 0 \\
\mathbf{e}_2 : \dfrac{dQ_{02}}{d\varepsilon} + Q_{1*}\dfrac{M_{03}}{A_{33}} + \kappa_{3*}Q_{01} + \Delta q_2 = 0 \\
\mathbf{e}_3 : \dfrac{dM_{03}}{d\varepsilon} + Q_{02} - h\Delta q_1 = 0
\end{cases}
\tag{16a}
$$

$$
\begin{cases}
\mathbf{e}_1 : \dfrac{dM_{01}}{d\varepsilon} - M_{3*}\dfrac{M_{02}}{A_{22}} - \kappa_{3*}M_{02} + h\Delta q_1 = 0 \\
\mathbf{e}_2 : \dfrac{dM_{02}}{d\varepsilon} + M_{3*}\dfrac{M_{01}}{A_{11}} + \kappa_{3*}M_{01} + Q_{03} = 0 \\
\mathbf{e}_3 : \dfrac{dQ_{03}}{d\varepsilon} + Q_{2*}\dfrac{M_{01}}{A_{11}} - Q_{1*}\dfrac{M_{02}}{A_{22}} + \Delta q_3 = 0
\end{cases}
\tag{16b}
$$

We assume further, that $q_i = 0$. System (16) resolves into two independent systems: (16a) and (16b). For determination of a critical load, under which the beam loses stability in the plane of the drawing, it is sufficient to consider system (16a). The system (16b) makes it possible to determine a critical load, under which the loss of stability occurs out-of-plane. For this purpose, parameters Q_1, Q_2, M_3 and κ_3 from system (11) are found at first from (11), and then they are used in system (16) with boundary conditions:

$$
Q_{01}(l) = 0 \qquad Q_{02}(l) = \delta \qquad Q_{03}(l) = \delta \qquad M_{01}(l) = 0 \qquad M_{02}(l) = 0 \qquad M_{03}(l) = 0 \tag{17}
$$

where δ is any small perturbation acting on a beam. If the solution of systems (16a) and (16b), describing the changes of the form of a beam (for example, $\Delta\kappa_3$ and $\Delta\kappa_2$), is comparable with the perturbation δ, then the equilibrium state of a beam is stable, otherwise - unstable.
The experimental results show good quantitative correspondence to the theoretical model.

4 Discussion and Conclusion

We have shown that the theory of curved beams is suitable for a quantitative and qualitative analysis of such structures. The particularity of this model is that the position of the neutral line in the beams is known and predefined (Figure 2) 2d) 3d)). The model allows for large elastic deformations and takes the mechanical and geometrical properties into account.
The results of the stability analysis provide information about critical loads and help to avoid unstable positions in such structures.
For the further development of the material coherent joints a cooperation is planned.

Acknowledgements

The authors wish to thank Prof. J. Steigenberger (TU Ilmenau) for his advice on mechanical problems. Also, the author would like to thank Dipl.-Biol. M. Karner (FSU Jena) for numerous consultations on biology. The work was supported by the Deutsche Forschungsgemeinschaft (INK 22/A1 and PE 693/1-1).

Literature

1. Blickhan, R.: Dehnungen im Außenskelett von Spinnen, Dissertation, Saarbrücken, (1983).

2. Blickhan, R.; Barth, F.G.: Strains in the exoskelett of spiders, J. Comp. Physiol. A (1985) 157, (1985), 115-147.

3. Foelix, R.F.: Biologie der Spinnen, Georg Thieme Verlag, (1992).

4. Karner, M.: Restriction in the evolution of arthropoid joints, in this volume, (1998).

5. Love, A.E.: Treatise on the Mathematical Theory of Elasticity, 4th Edition, Published by Dover Pubns, (1927).

6. Lauschke, U.: Analyse und Simulation des mechanischen Verhaltens faserarmierter, mehrlumiger Druckschlauchstrukturen, Dissertation, Otto-von-Guericke Universität Magdeburg, (1997).

7. Parry, D.A.; Brown, H.J.: The hydraulic mechanism of the spider leg. J. exp. Biol. 36, (1959), 423-433.

8. Parry, D.A; Brown, H.J.: The jumping mechanism of salticid spider, Journal of experimental biology, (1959).

9. Svetlickii, V.A.: Mechanika sterschnei, Moskva, "Visschaja Schkola", (1987).

10. Wilson, R.S.: Some comments on the hydrostatic system of spiders (Chelicerata, Araneae). Z.Morf. Tiere 68, (1970), 308-322.

Addresses: Dr. Lena Zentner, Technical University Ilmenau, Institute of Mechanical Engineering, D-98684 Ilmenau, Germany; Dr. Sergey Petkun, Prof. Dr. Reinhard Blickhan, Friedrich-Schiller-University Jena, Institute of Sports Science Biomechanics Group, D-07740 Jena, Germany.